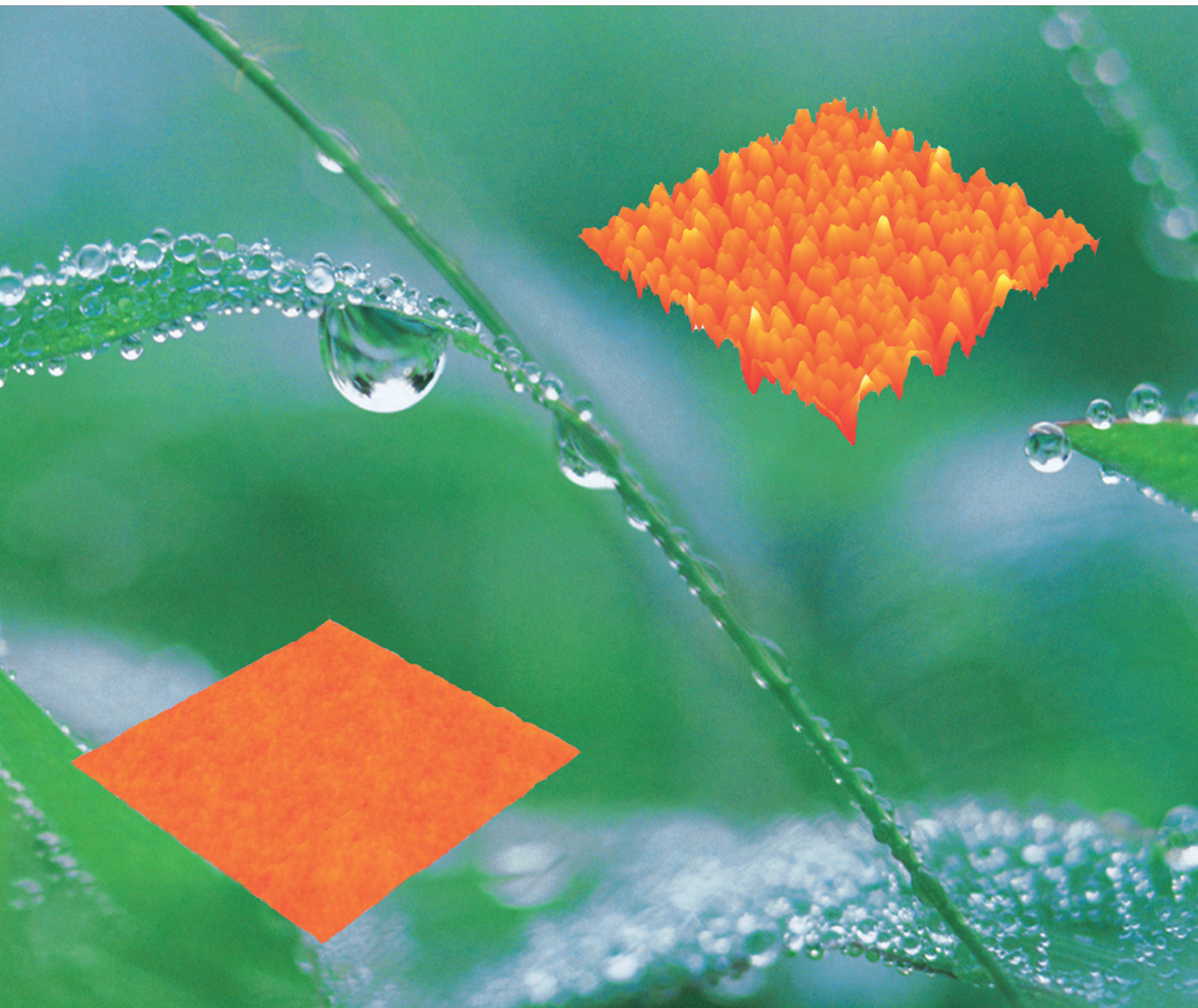


ChemComm

Chemical Communications

www.rsc.org/chemcomm

Number 2 | 14 January 2008 | Pages 125–264



ISSN 1359-7345

COMMUNICATION

Wei Chen, Liangti Qu, Dongwook Chang, Liming Dai, Sabyasachi Ganguli and Ajit Roy

Vertically-aligned carbon nanotubes infiltrated with temperature-responsive polymers: smart nanocomposite films for self-cleaning and controlled release

RSC Publishing

Vertically-aligned carbon nanotubes infiltrated with temperature-responsive polymers: smart nanocomposite films for self-cleaning and controlled release†

Wei Chen,^a Liangti Qu,^a Dongwook Chang,^a Liming Dai,^{*a} Sabyasachi Ganguli^b and Ajit Roy^b

Received (in Cambridge, UK) 1st October 2007, Accepted 31st October 2007

First published as an Advance Article on the web 9th November 2007

DOI: 10.1039/b715079b

We have demonstrated that the infiltration of temperature-responsive polymers (e.g., PNIPAAm) into vertically-aligned carbon nanotube forests created synergetic effects, which provided the basis for the development of smart nanocomposite films with temperature-induced self-cleaning and/or controlled release capabilities.

Owing to their unique mechanical, electronic, and thermal properties attractive for a large variety of potential applications, carbon nanotubes have received considerable attention since Iijima's report in 1991.^{1,2} In particular, carbon nanotubes have been widely investigated as reinforcement fillers for developing advanced polymer nanocomposites with ultrahigh strength/weight ratios and superior electrical/thermal properties.³ Although the majority of studies on polymer and carbon nanotube nanocomposites have so far focused on *non-aligned* carbon nanotubes, a few recent studies on advanced nanocomposites based on polymers and *vertically-aligned* carbon nanotubes have clearly demonstrated their great promise with synergetic effects. Potential applications of the vertically-aligned multiwalled carbon nanotube (VA-MWNT) and polymer nanocomposites include flexible electronics,⁴ actuators,⁵ functional membranes,⁶ Gecko-foot-mimetic dry adhesives,⁷ and biological/chemical sensors,⁸ to mention but a few. For many of these and other applications, it is highly desirable for the aligned carbon nanotube and polymer nanocomposites to possess *self-cleaning* (e.g. as antifouling substrates, artificial Gecko feet) and *controlled release* (e.g. as functional membranes, sensors) capabilities. These smart nanocomposites and nanodevices can be devised by judiciously compositing vertically-aligned carbon nanotubes with various stimuli-responsive polymers.⁹

Poly(*N*-isopropylacrylamide) (PNIPAAm) is the most widely studied temperature-responsive polymer, which undergoes a rod-coil conformational transition in an aqueous medium around the lowest critical solution temperature (LCST \approx 32 °C).⁹ By infiltrating the PNIPAAm polymer gel into the VA-MWNT forest, we report here a novel concept for developing a new class of smart nanocomposite films with self-cleaning and/or controlled release properties originating from the temperature-responsive

PNIPAAm chains partially expanding out from the nanotube gaps as dangling chains at the VA-MWNT/liquid interface.

Fig. 1 shows a schematic of the procedure used to prepare the PNIPAAm/VA-MWNT smart nanocomposite films (see ESI for details†). Briefly, VA-MWNTs were produced by pyrolyzing iron(II) phthalocyanine (FePc)^{10a} onto a silicon wafer. The resultant VA-MWNT array was then set up for the uptake of the potassium persulfate initiator (Sigma-Aldrich) (Fig. 1a & S1a†),¹¹ *N*-isopropylacrylamide (NIPAAm) monomer (Sigma-Aldrich, purified by recrystallization), and *N,N'*-methylenebisacrylamide crosslinker (BIS, Sigma-Aldrich) (Fig. 1b), followed by addition of *N,N,N',N'*-tetramethylethylenediamine (TEMED) accelerator (Sigma-Aldrich) to co-initiate the free radical polymerization (Fig. 1c & S1b,c†). Thereafter, the infiltrated PNIPAAm chains were further confined by an epoxy coating after selective water-plasma-etching^{6,12} of PNIPAAm to expose the nanotube tips for good contact with the epoxy layer (Fig. 1d & e). The epoxy sealant was used to ensure that the confined PNIPAAm chains expand/shrink along the nanotube length direction (*vide infra*). Finally, the epoxy-sealed PNIPAAm/VA-MWNT nanocomposite film was removed from the Si wafer in an aqueous solution of HF (10 wt%)^{10a} and inverted (Fig. 1f) for slightly etching the infiltrated PNIPAAm chains by the water-plasma to expose the VA-MWNTs (Fig. 1g & S1d†). As a reference, a similar VA-MWNT film infiltrated with the temperature-insensitive epoxy resin was also prepared.

Along with a SEM examination to follow the above procedure in the dry state (Fig. S1†), atomic force microscopy (Veeco Explorer AFM) was also used to investigate the top surface of the pristine VA-MWNT array (Fig. 2a) and PNIPAAm/VA-MWNT

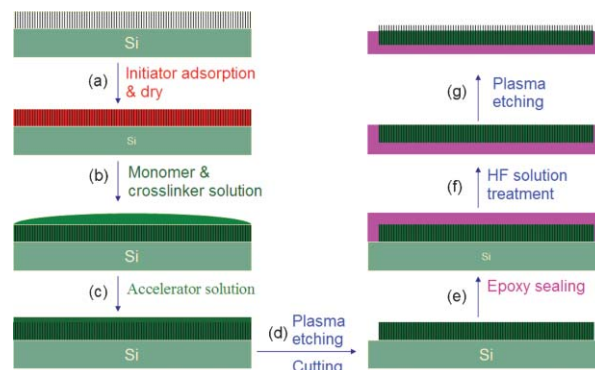


Fig. 1 Schematic illustration of the procedure for fabricating the smart PNIPAAm/VA-MWNT nanocomposite films.

^aDepartment of Chemical and Materials Engineering, University of Dayton, Dayton, OH 4546, USA. E-mail: ldai@udayton.edu; Fax: +1 937 229 3433; Tel: +1 937 229 2670

^bAir Force Research Laboratory, Materials and Manufacturing Directorate, Wright-Patterson AFB, OH 45433, USA

† Electronic supplementary information (ESI) available: Experimental details. Fig. S1, S2, & S3. See DOI: 10.1039/b715079b

nanocomposite film (Fig. 2b & c) both in the dry and a wet state at room temperature (20 °C). Fig. 2a shows a uniform nanotube length and surface density for the pristine VA-MWNT array whereas the dry surface of the PNIPAAm/VA-MWNT film (Fig. 2b) clearly shows features associated with the water-induced VA-MWNT bundles^{10b} extruding out from the PNIPAAm matrix up to ~300 nm after the preferential plasma etching of the infiltrated PNIPAAm chains. To check the surface topology in a wet state, we prepared a wet sample by submersing the PNIPAAm/VA-MWNT nanocomposite film in water for 5 minutes at room temperature prior to the AFM imaging. The much smoother featureless surface, with a reduced roughness of ~10 nm, shown in Fig. 2c is an indication that the infiltrated PNIPAAm chains had expanded out from the gaps in the VA-MWNT forest to cover the nanotube top surface. Fig. 2d–f schematically show the above process. While the plasma etching preferentially removed the top polymer layer in order to expose the aligned MWNTs from the PNIPAAm matrix (*cf.* Fig. 1g, 2d & S1d†), the hydrated PNIPAAm polymer chains undertook the extended conformation below the LCST (Fig. 2e) and the collapsed conformation above the LCST (~32 °C)⁹ (Fig. 2f) in an aqueous solution. The expanding PNIPAAm chains can not only repel objects away from the nanotube top surface for self-cleaning to remove contaminants adsorbed onto the VA-MWNT film but also provide an effective means for controlled release of objects trapped within the infiltrated PNIPAAm chains, as discussed below.

In view of the ease with which gold nanoparticles can be visualized on SEM and characterized by their surface plasmon resonance absorbance,¹³ we chose gold nanoparticles as model “contaminants” to demonstrate the self-cleaning capability of these PNIPAAm/VA-MWNT nanocomposite films. To start with, we immersed the PNIPAAm/VA-MWNT nanocomposite film

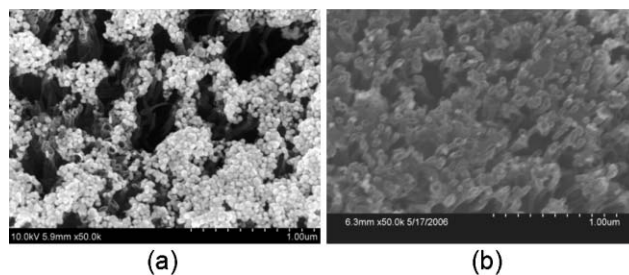


Fig. 3 SEM images of the PNIPAAm/VA-MWNT nanocomposite film (a) after adsorbing gold nanoparticles on its top surface from an aqueous solution at 50 °C and (b) after removal of the adsorbed gold nanoparticles by reducing the solution temperature down to 25 °C.

into an aqueous solution of gold nanoparticles¹³ (*ca.* 20–50 nm in diameter, ESI†) at 50 °C to allow for adsorption of the nanoparticles onto the nanotube top surface (Fig. 3a). By simply reducing the solution temperature down to 25 °C (<LCST ≈ 32 °C) (Fig. 3b), we found that almost all of the pre-adsorbed gold nanoparticles were dissociated from the top surface of the PNIPAAm/VA-MWNT nanocomposite film.

The temperature-induced PNIPAAm conformation transition shown in Fig. 2e & f is clearly responsible for the above observed self-cleaning process as the expanded chains at 25 °C (Fig. 2e) can physically “push” the pre-adsorbed nanoparticles off from the nanotube top surface. A trivial explanation of the observed nanoparticle removal related to possible weak adsorption of gold nanoparticles on the aligned nanotube array can be ruled out based on the fact that the nanoparticle adsorption–cleaning was reversible in the aqueous solution by changing temperatures between 50 and 25 °C. Additionally, gold nanoparticles adsorbed onto the epoxy/VA-MWNT reference film (Fig. S3a†) under the same conditions could not be removed by decreasing the

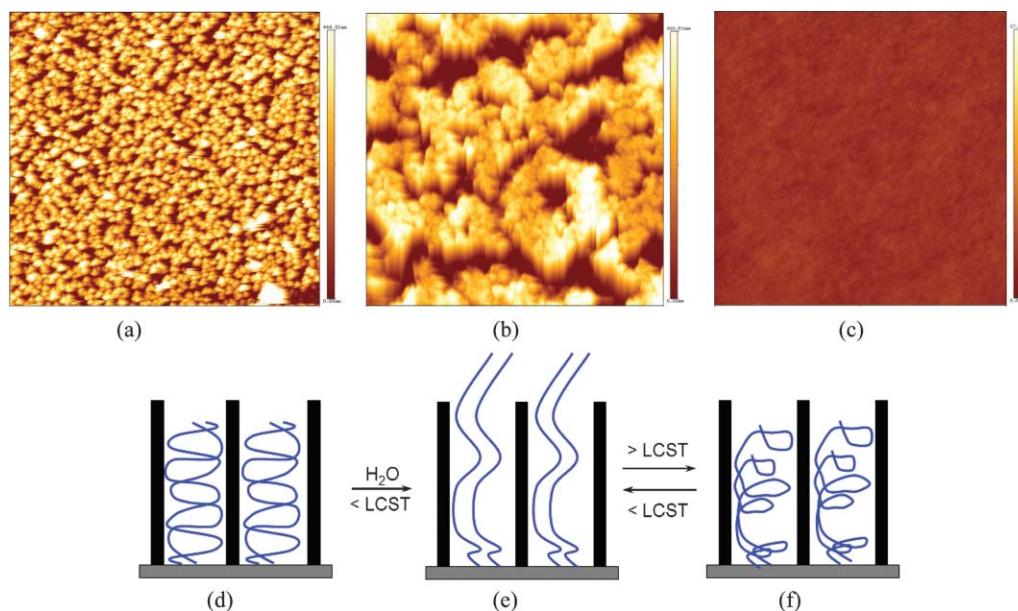


Fig. 2 Tapping mode AFM images of (a) a pristine VA-MWNT array; and the PNIPAAm/VA-MWNT nanocomposite film: (b) in the dry state and (c) in the wet state. *x*–*y*–Scale: (a–c) 5 μm × 5 μm, *z*–scale: (a) 445 nm; (b) 667 nm; (c) 17 nm. A schematic representation of the PNIPAAm/VA-MWNT film: (d & e) in the dry and wet state, respectively, at room temperature (20 °C), and (f) in the wet state at a temperature above the LCST (~32 °C). For clarity, the infiltrated polymer mesh is represented by a few long polymer chains.

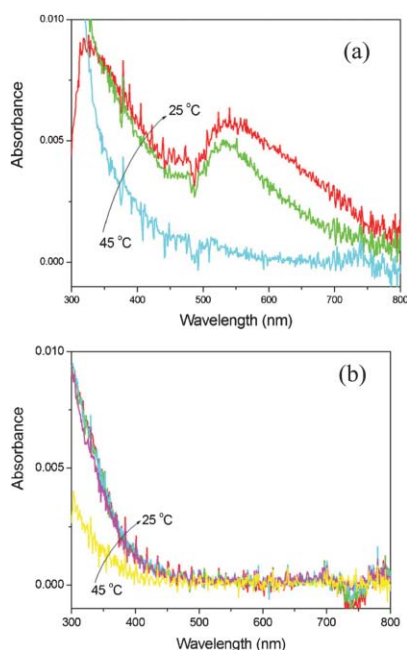


Fig. 4 UV/Vis spectra of aqueous media containing (a) a gold-nanoparticle-intercalated PNIPAAm/VA-MWNT (blue) and (b) a gold-nanoparticle-intercalated epoxy/VA-MWNT nanocomposite film (yellow) at 45 °C, both followed a reduction of the temperature to 25 °C (green) and a second cycle from 25 °C → 45 °C → 25 °C (red).

temperature down to or even below 25 °C in a control experiment (Fig. S3b†). Besides, no obvious adsorption–desorption of gold nanoparticles was observed for a pure PNIPAAm film, while gold nanoparticles adsorbed on the pristine aligned carbon nanotube array remained under the same temperature-change cycles. Therefore, it is the unique combination of the temperature-responsive PNIPAAm and the aligned carbon nanotube forest that makes the self-cleaning possible. In addition to the gold nanoparticles used above for easy SEM imaging, the self-cleaning concept thus demonstrated could be applicable for cleaning many other surface “contaminants”, ranging from dust particles to proteins. Furthermore, the same principle can also be exploited for controlled release applications, indicating multifunctionality for the PNIPAAm/VA-MWNT nanocomposite films.

To demonstrate the controlled release concept, we followed the same procedure as that shown in Fig. 1, but mixed the gold nanoparticles, having a surface plasmon resonance peak at ~530 nm (*vide supra*), in the NIPAAm monomer to be infiltrated into the gaps of the VA-MWNT forest at step b of Fig. 1. The nanoparticle-containing PNIPAAm/VA-MWNT composite film was then immersed into pure water at 45 °C (>LCST) for about 3 min to reach equilibrium. Upon cooling down to 25 °C (<LCST), the PNIPAAm chains undertook the extended structure and expanded beyond the aligned nanotube top surface, quickly releasing nanoparticles into the liquid phase (typically, <1 min). The newly-released gold nanoparticles were readily monitored by measuring the increase in the solution optical absorption intensity around 530 nm (PerkinElmer Lambda 900 UV/VIS/NIR spectrometer), as shown in Fig. 4a. Within the subsequent temperature-change cycle(s), the surface plasmon resonance peak characteristic

of the gold nanoparticles further increased, albeit slightly due to a low releasing dose in this particular case. In contrast, there is no surface plasmon resonance peak at 530 nm in the corresponding UV/Vis spectra recorded on an epoxy/VA-MWNT reference composite film containing gold nanoparticles under the same conditions (Fig. 4b).

In summary, we have demonstrated for the first time that the infiltration of temperature-responsive polymers into vertically-aligned carbon nanotube forests created synergetic effects, which provided the basis for the development of smart nanocomposite films with temperature-induced self-cleaning and controlled release capabilities. It is the temperature-induced reversible rod–coil conformational transition of PNIPAAm in an aqueous solution that enables the infiltrated polymer chains to expand out or collapse within the nanotube gaps for self-cleaning and controlled release actions. With so many stimuli (*e.g.* temperature, solvent, pH, photo, ionic, electrical) responsive polymers already developed, and more to be synthesized, we believe that our concept represents a versatile means to develop various functional polymer and aligned carbon nanotube-based multifunctional smart nanocomposite materials and devices with switchable surface characteristics.

We thank Rachel Smith and Qiwen Zhan for help. LD thanks the support from AFOSR (FA9550-06-1-0384) and NSF (CMS-0609077, 0708055).

Notes and references

- 1 S. Iijima, *Nature*, 1991, **354**, 56–58.
- 2 *Carbon Nanotechnology: Recent Developments in Chemistry, Physics, Materials Science and Device Applications*, ed. L. Dai, Elsevier, Amsterdam, 2006.
- 3 (a) R. H. Baughman, A. A. Zakhidov and W. A. de Heer, *Science*, 2002, **297**, 787–789; (b) E. T. Thostenson, Z. F. Ren and T. W. Chou, *Compos. Sci. Technol.*, 2001, **61**, 1899–1912.
- 4 Y. J. Jung, S. Kar, S. Talapatra, C. Soldano, G. Viswanathan, X. S. Li, Z. L. Yao, F. S. Ou, A. Avadhanula, R. Vajtai, S. Curran, O. Nalamasu and P. M. Ajayan, *Nano Lett.*, 2006, **6**, 413–418.
- 5 S. V. Ahir and E. M. Terentjev, *Nat. Mater.*, 2005, **4**, 491–495.
- 6 B. J. Hinds, N. Chopra, T. Rantell, R. Andrews, V. Gavalas and L. G. Bachas, *Science*, 2004, **303**, 62–65.
- 7 (a) B. Yurdumakan, N. R. Ravavikar, P. M. Ajayan and A. Dhinojwala, *Chem. Commun.*, 2005, 3799–3801; (b) L. Ge, S. Sethi, L. Ci, P. M. Ajayan and A. Dhinojwala, *Proc. Natl. Acad. Sci. U. S. A.*, 2007, **104**, 10792–10795; (c) L. Qu and L. Dai, *Adv. Mater.*, 2007, DOI: 10.1002/adma.200700023.
- 8 (a) C. Wei, L. Dai, A. Roy and T. B. Tolle, *J. Am. Chem. Soc.*, 2006, **128**, 1412–1413; (b) C. V. Nguyen, L. Delzeit, A. M. Cassell, J. Li, J. Han and M. Meyyappan, *Nano Lett.*, 2002, **2**, 1079–1081.
- 9 (a) L. Dai, *Intelligent Macromolecules for Smart Devices: From Materials Synthesis to Device Applications*, Springer-Verlag, New York, 2004; (b) H. G. Schild, *Prog. Polym. Sci.*, 1992, **17**, 163–249; (c) L. Ionov, M. Stamm and S. Diez, *Nano Lett.*, 2006, **6**, 1982–1987.
- 10 (a) S. Huang, L. Dai and A. W. H. Mau, *J. Phys. Chem. B*, 1999, **103**, 4223–4277; (b) S. H. Li, H. J. Li, X. B. Wang, Y. L. Song, Y. Q. Liu, L. Jiang and D. B. Zhu, *J. Phys. Chem. B*, 2002, **106**, 9274–9276.
- 11 C. Erbil, Y. Yildiz and N. Uyanik, *Polym. Int.*, 2000, **49**, 795–800.
- 12 S. Huang and L. Dai, *J. Phys. Chem. B*, 2002, **106**, 3543–3545.
- 13 (a) J. J. Storhoff, R. Elghanian, R. C. Mucic, C. A. Mirkin and R. L. Letsinger, *J. Am. Chem. Soc.*, 1998, **120**, 1959–1964; (b) S. Stoeva, A. B. Smetana, C. M. Sorensen and K. J. Klabunde, *J. Colloid Interface Sci.*, 2007, **309**, 94–98; (c) L. Qu, L. Dai and E. Osawa, *J. Am. Chem. Soc.*, 2006, **128**, 5523–5532; (d) P. Jiang, J. J. Zhou, R. Li, Z. L. Wang and S. S. Xie, *Nanotechnology*, 2006, **17**, 3533–3538; (e) F. Kim, S. Connor, H. Song, T. Kuykendall and P. D. Yang, *Angew. Chem., Int. Ed.*, 2004, **43**, 3673–3677.